SLAC-PUB-2563
July 1980
(T/E)

e^+e^- PHYSICS NEAR CHARM THRESHOLD VIA THE CRYSTAL BALL*

D. G. Coyne
(Representing the Crystal Ball Collaboration)[1]
Stanford Linear Accelerator Center
Stanford University, Stanford, California 94305

and

Princeton University, Princeton, New Jersey 08540

ABSTRACT

We discuss the use of the Crystal Ball detector for the study of e^+e^- annihilations near charm threshold: at the $\psi(3097)$, $\psi'(3685)$, $\psi''(3770)$ and in the "continuum" $3770 \leq \sqrt{s} \leq 4500$ MeV. This paper will concentrate on the special techniques available to the Crystal Ball which allow measurement of inclusive γ, π^0 and η cross sections. Preliminary results for these processes at particular center of mass energies are presented. An update of the inclusive and exclusive evidence for the $\eta_c(2980)$, for the sake of completeness, is given in the Appendix.

I. INTRODUCTION

The use of the Crystal Ball detector in the study of the "continuum" region just above charm threshold introduces a number of unfamiliar but useful techniques in e^+e^- physics. The major purpose of this report is to outline those techniques and to discuss areas of pertinence where they will be applied. Another purpose is to present our preliminary results in some of these areas, based on first analyses of partial data samples.

The organization of this report is to describe the detector briefly, and to make a short survey of the state of knowledge of the continuum prior to the Crystal Ball measurements. After an outline of the strategy of data-taking we have used, we present results of the Crystal Ball "baseline" measurements, i.e., the proof of the ability to measure inclusive γ, π^0 and η signals at c.m. energies below charm threshold and/or on- ψ resonances. The resolutions and efficiencies for these modes are discussed. We then move above charm threshold and into the "continuum" region (which itself appears to have imbedded ψ-like resonances). The report concludes

* Supported in part by the Department of Energy, contract DE-AC03-76SF00515, and by National Science Foundation Grant PHY79-16461.

(Invited talk presented at the Vanderbilt Symposium on High Energy e^+e^- Interactions, Nashville, Tennessee, May 1-3, 1980.)

with our preliminary measurements of selected inclusive modes at interesting c.m. energies.

II. THE DETECTOR

The Crystal Ball is a fieldless, segmented spherical shell of NaI(Tℓ) surrounding chambers having charged-particle tracking capabilities. The detector, built and operated by the Crystal Ball Collaboration,[1] is shown diagrammatically in Fig. 1. A detailed description of the apparatus is given elsewhere;[2] for the purposes of this discussion there are several crucial parameters.

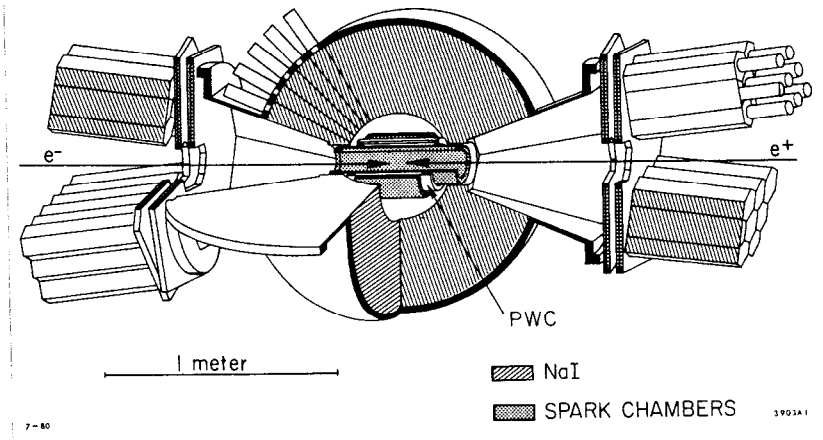

Figure 1. Schematic cutaway view of the Crystal Ball detector.

A) The energy resolution for photons in the Ball itself (as opposed to the endcaps) is $\sigma_E/E_\gamma \approx 3\%/E_\gamma^{1/4}$ with E_γ in GeV. This holds well for 50 MeV $\leq E_\gamma \leq$ 2 GeV and leads to a Γ(FWHM) of about 10% of E_γ in the regions of interest. This resolution is available over ~ 85% of 4π radians.

B) The angular resolution for photons is determined by the segmentation of the NaI (720 segments over the complete sphere) and by weighting the crystal segments according to the energy deposition within each participating crystal of a photon shower. This gives $\sigma_{\theta_\gamma} \approx 1$ to 2°, depending on the range of photon energies. (θ_γ is a polar angle relative to the γ true direction.)

C) The angular resolution for charged particles is determined by the number of proportional wire chamber planes and magnetostrictive spark chamber planes through which it passed. We get $\sigma_{\theta_c} \approx .3 - 1^\circ$ depending on the geometry of the track, with smaller values pertinent for the 75% of the solid angle furthest from the endcaps.

The analysis modes most appropriate to this detector are measurement of inclusive γ, inclusive π^0, η and other states decaying into all-γ final states. In addition the Ball can overconstrain any event exclusively for any number of electromagnetically decaying secondaries in the final state, as long as the number of unabsorbed charged particles does not exceed 2. (Zero-constraint "fits" can allow 4 charged particles.) An example of these modes was our detection of a candidate state for η_c in inclusive and exclusive states, as summarized in the Appendix.

We have developed algorithms for the recognition of final-state photons and charged particles, together with cuts designed to take advantage of the portions of the Ball and the event topologies where the best measurements are available. Our general approach is to use highly cut data for the search for new effects, and relatively uncut data to arrive at numerical results in the least-biased manner possible.

The major complication of the analysis of data from this detector is pattern recognition in the presence of strongly interacting particles and shower fluctuations. Residuals from untagged charged particles (at the level of a few percent) also complicate the analysis.

Our basic check of the credibility of the cuts and subsequent pattern recognition is the ability of the detector to reproduce standard QED distributions involving e's and γ's with absolute normalization.[3]

III. STATE OF KNOWLEDGE OF THE CONTINUUM (PRE-CRYSTAL BALL)

While we cannot do justice here to the many papers published concerning the effects within the continuum, we can mention those areas of study most likely to be investigated by the Crystal Ball.

The global behavior of the cross section $e^+e^- \rightarrow$ hadrons has been studied by most of the past detectors at e^+e^- storage rings. A representative sample[4] is shown in Fig. 2. Absolute differences of the order of 20% in R are evident, and point-to-point systematics clearly dominate the statistical errors. Nonetheless, certain features are

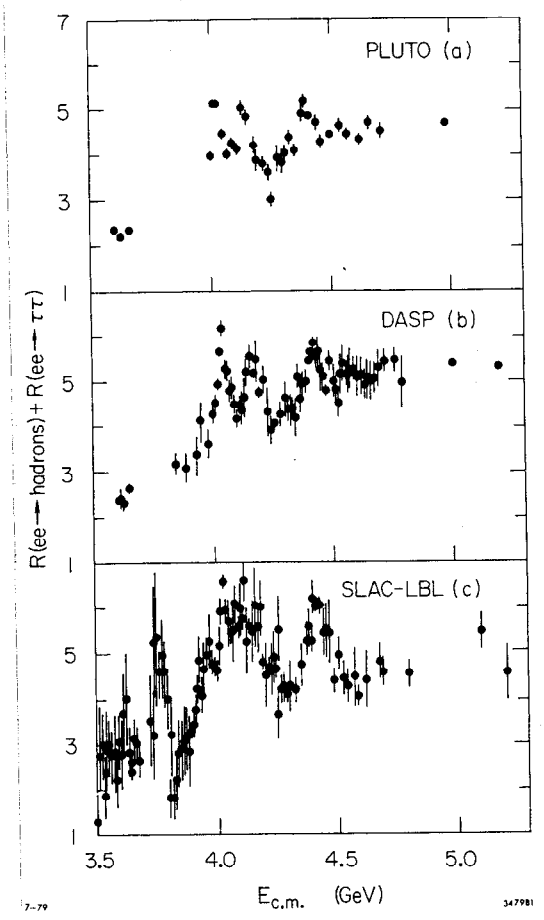

Fig. 2. $R = \sigma(e^+e^- \to \text{hadrons})$ $\sigma(e^+e^- \to \mu^+\mu^-)$ as measured by three detectors in the region $\sim 3.7 < \sqrt{s} < \sim 4.6$ GeV. Radiative corrections but none for τ have been applied (Ref. 4).

invariably present in all samples, such as the $\psi''(3770)$ (when measured), the "D^*" resonance at ~4.03 GeV, and the large bump at ~4.4 GeV. Often but not invariably present are suggestive structures at 3.9 GeV, 4.16 GeV, and details of the rapid fall after 4.2. While the global variations in R are presumed to be related to variations in D production[5] there is no clear picture of the fine structure (if any) of R nor of small processes which may occur in addition to D production.

The existence of thresholds for charmed particles in this region has been a fruitful topic of study. The D's have been studied most intensely, though not exhaustively, at the $D\bar{D}$-factory $\psi''(3770)$ in exclusive final states.[6,7] Of more pertinence to this report are the studies of D and D^* performed at $\sqrt{s} = 4.028$ in quasi-inclusive modes, in which the $D^{\pm}$ or D^0 is detected and fit from its $K\pi$ or $K\pi\pi$ modes and the spectra of momenta recoiling against the D is used to deduce parameters of the system: D^* masses, $D^* \to D\gamma$ branching ratio, $D^*\bar{D}^* : D^*\bar{D} + D\bar{D}^*$ production ratios, charged D ratios, etc.[8] Figure 3 shows how the recoil momentum spectrum is affected by the possible variation of these parameters. The method is fairly direct for some of the parameters (such as production ratios) but quite indirect for the D^*-D Q-value and γ branching ratio. The data are slim statistically, but rather good numbers on some of the parameters nonetheless emerge (see the later comparison

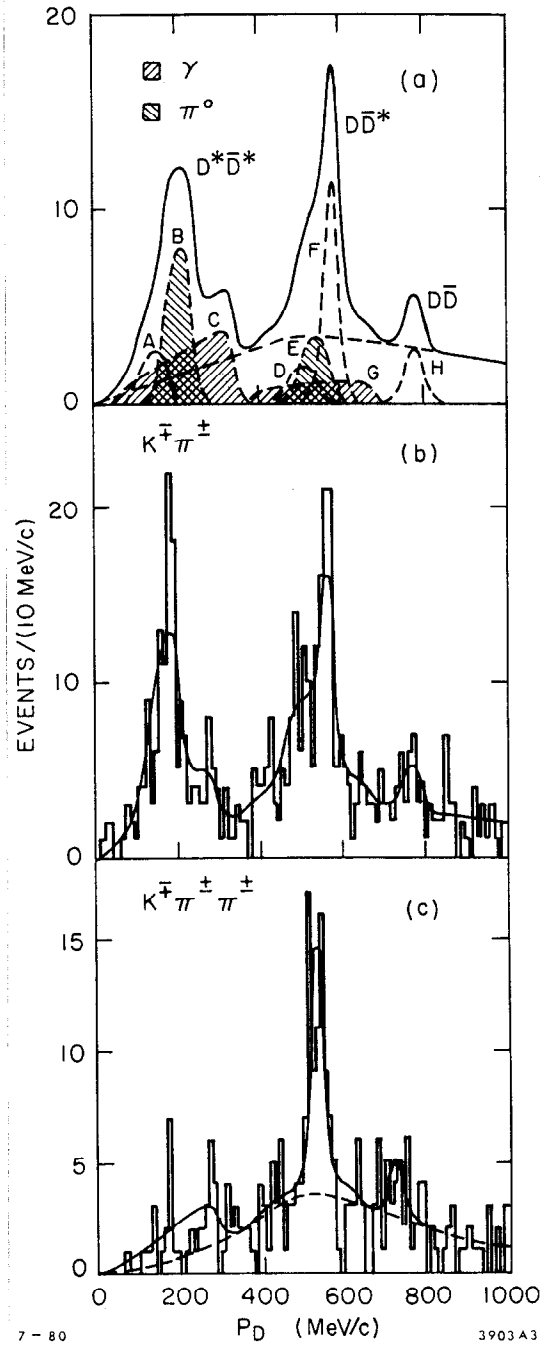

Fig. 3. Parameter fitting with D recoil momenta studies (Ref. 8).

Table III). Figure 4 shows the energy level scheme[9] underlying these spectra.

The situation for strange-charmed mesons, the F/F*, is much less well-defined. In e^+e^- storage ring investigations, the main evidence for the F comes from two largely independent results of the DASP collaboration.[10,11] The first result, Fig. 5, is that the inclusive cross section for η appears to have one or more thresholds in the vicinity of $\sqrt{s} = 4.16$ and 4.4 GeV. The experiment placed tight limits on the inclusive η cross section at $\sqrt{s} = 4.03$, thus suggesting that neither D's nor non-charm background was an appreciable source of η's; this implied that the eventual appearance of η's was likely evidence for F's, which are expected to have ≈50% of their decays into final states involving an η.[12] Correlations with electrons and low energy γ's (expected from $F^* \rightarrow \gamma F$) strengthened this interpretation. The second result, Fig. 6, was a cluster of events at $\sqrt{s}$ = 4.42 GeV fitting the exclusive hypothesis $e^+e^- \rightarrow F^*F$ or F^*F^* giving unique masses for F and F* as shown. There are a number of recent results[13] with candidates for F's with a similar mass, and even a lifetime measurement! In this report of Crystal Ball results, we

Fig. 4. The energy level scheme for D^* decays (Ref. 9).

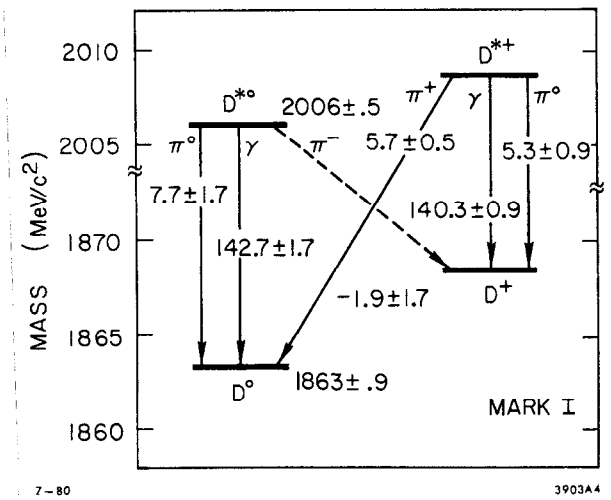

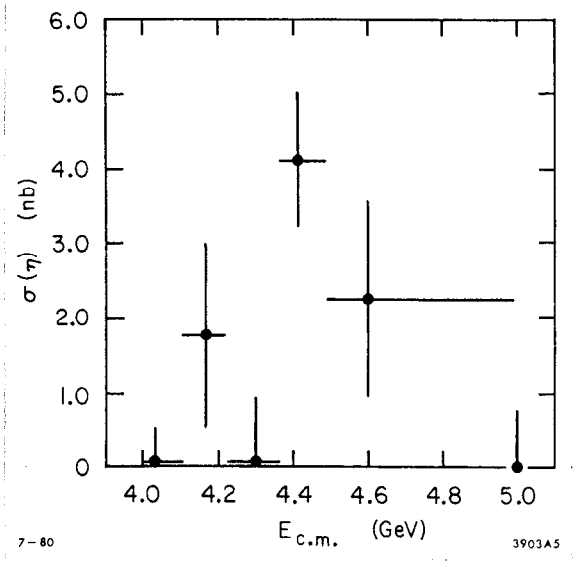

Fig. 5. The η-inclusive cross section (DASP, Ref. 10).

will consider only the η-clusive measurement and its interpretation. Limits on the transition $F^* \rightarrow \gamma F$ and a search for the F via the analogous exclusive modes in the Ball are in preparation and will be discussed in future reports.

Before leaving this subject, we should note that there are several other possible thresholds expected in the range $3.8 < \sqrt{s} < 4.5$ GeV.

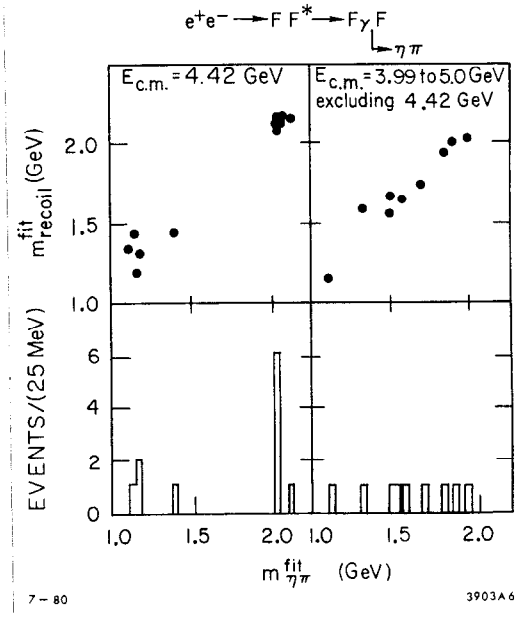

Fig. 6. Exclusive candidates for F,F^* (DASP,Ref. 11).

Figure 7 shows a prediction[14] of the locations of the P-wave excitations of the charmed and strange-charmed mesons, D^{**} and F^{**}. As an example, the threshold for DD^{**} production is ~4.1 GeV and for FF^{**} is ~4.4 GeV. Thus we might expect that if the inclusive modes are examined in detail, many spectral lines characteristic of these γ, π^0, $2\pi^0$, η and K transitions

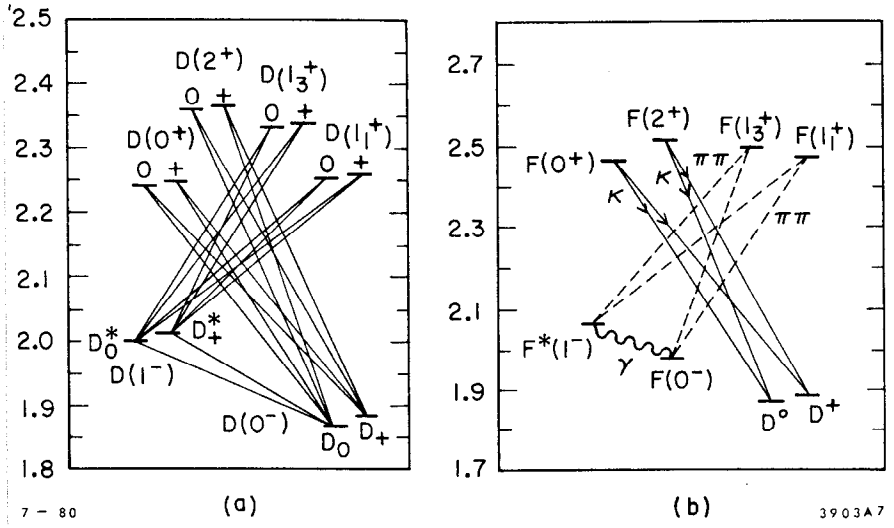

Fig. 7. The energy level scheme predicted for charmed and strange-charmed mesons (Ref. 14).

may be present near the respective thresholds, albeit with small intensities. The detection of such processes and the location of "factories" for new states, if any, are thus outstanding problems in this energy region.

The effect of the possible thresholds on the cross section is in itself an interesting physics question. There exist preliminary theoretical models of the effect of imbedding psi-like resonances in the continuum; the coupled-channel model[15] gives cross sections which are critically dependent on the number and position of thresholds for charmed and strange-charmed mesons. Stated briefly (and imprecisely), the transition of an imbedded psion into two specific mesons is constrained by spin-parity to particular relative angular momenta between the mesons; it is constrained by the masses involved and by $\sqrt{s}$ to particular values of the relative linear momentum between the mesons. This implies that the rate of production of such meson pairs is sensitive to the nodes and antinodes of the spacial wave function of the psion (or to the momentum-space analog). Therefore relatively small changes in $\sqrt{s}$ can make large changes in the $p_{relative}$ of the meson pair near threshold, with concurrent large changes in production rate of meson pairs. The psion channels

are coupled in that overlap integrals between two psions interacting through exchanges of the mesons are involved.

This picture seems qualitatively right, but neither theory nor data yet exists in a form adequate for a precise test.[16] Figure 8 shows the quantitative prediction for a model involving D, D^*, F, F^* only. (Masses are taken to be experimental values from SLAC/LBL and DASP). Note that $D^*\bar{D}^*$ and $D^*\bar{D}+D\bar{D}^*$ production dominate the region $3.9 < \sqrt{s} < 4.5$ GeV, with no factories expected for F or F^* and cross sections $\leq .2$ nb. The highest signal/noise for F is expected at the minimum R, $\sqrt{s} \approx 4.25$ GeV. This model can be used as an experimental guide to the rates expected, or inversely, the data can help define what states must be present in the model.

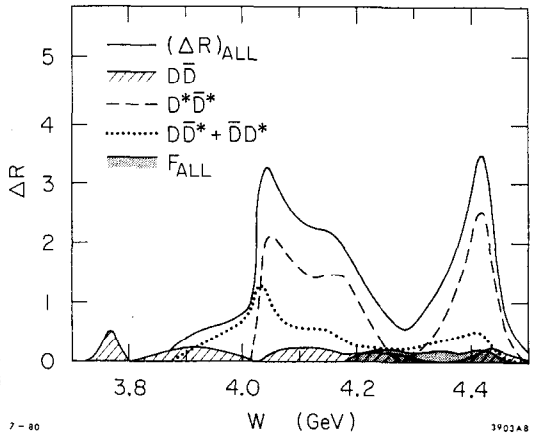

Fig. 8. The partial cross sections expected for production of specific meson pairs (Ref. 15).

Finally, the study of the imbedded states in the continuum for their own sake is of great interest for the testing of models of quark interactions. The quantum numbers, positions and decay properties of the imbedded states should help determine if they are "simple" $q\bar{q}$ resonances (potential model), complex multi-quark states (molecular models) or excitations of the gluon string (vibrational states). An example of a physical quantity testing such details is the angular distribution of the π^0 (relative to the beams) from $D^* \rightarrow \pi^0 + D^0$. It determines the ratio of spin amplitudes in the production of D^*D^*; there is a prediction for this at the $\psi(4028)$ based on resonance dynamics. For details of this theoretical application, see Cahn and Kayser and associated literature.[17]

In summary of this discussion, it is fair to say that the continuum region has had only a preliminary inspection and that many

opportunities for confrontation of theory and experiments still exist, dependent on the acquisition of informative data samples.

IV. THE CRYSTAL BALL AS A CONTINUUM DETECTOR: "BASELINE" MEASUREMENTS

A) A Strategy for Continuum Measurements.

We have seen that the collected data in the continuum are sparse; this stems from the fact that there is a relatively wide region, some 1000 MeV, in which new features can appear, but that these new features can persist or fluctuate over c.m. energy ranges as small as 20 MeV. The 4.028 resonance and its attendant structure is such a case. A simple calculation of the integral luminosity required to cover this continuum thoroughly, with sensitivity to phenomena with $\Delta R \approx .2$, yields run plans of about five years duration--a practical impossibility.

The approach used with the Crystal Ball detector is to scan the entire region, using inclusive distributions of γ, π^0, η and R to indicate regions of $\sqrt{s}$ with special interest, and then to rescan for confirmation of the effects. Finally, long fixed-energy runs are made at selected values of $\sqrt{s}$ to provide data sets for exclusive analysis. The calendar periods required for these three steps are about 5, 12 and 6 weeks, respectively. At present, we have finished the initial two scanning stages and one fixed energy (4.028). The data discussed below are mostly from the first stage and 4.028. Table I shows the integral luminosities corresponding to the various scan periods.

Table I: Integral Luminosities Collected by the Crystal Ball in a Scan Mode

Date	Energy Region	$\int \mathscr{L} dt (nb^{-1})$
May 1979	3.88-4.45 GeV	3092
Nov. 1979	3.67,4.03 GeV	300, 840
Mar. 1980	4.04-4.214 GeV	2875
June 1980	3.67,4.22-4.48 GeV	200, 2360
	Total	9667 nb^{-1}

This approach is not new; Fig. 9 shows some inclusive indicators used by Mark I[18] in similar scans. The mean multiplicity and charged energy fractions turned out to be insensitive indicators of changes in the underlying physics--the best indicator was R itself.

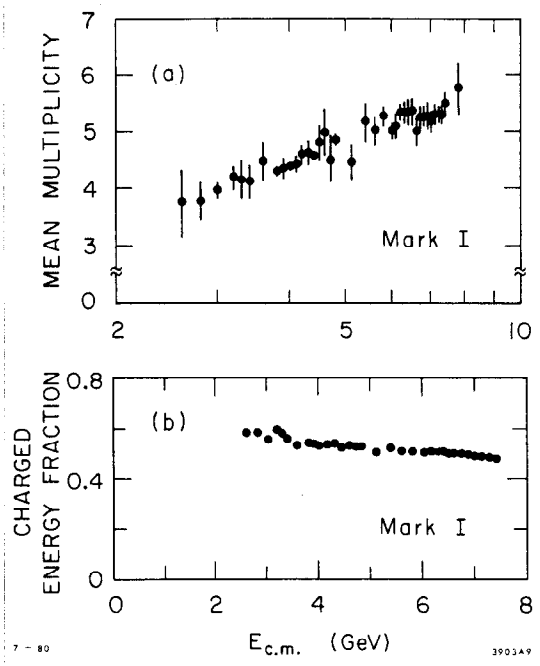

Fig. 9: Inclusive Quantities in the Mark I Scan Mode: a) charged energy fraction, b) mean multiplicity (Ref. 18).

What is new is that the Crystal Ball measures neutral-related quantities such as neutral energy fraction and neutral multiplicity. Fig. 10 shows that the former of these is again insensitive to changes in underlying physics, but that large changes in neutral multiplicity are seen.[19] This implies that the distributions of low-energy γ's, π^0's and η's could be useful indicators, and these were stressed in the scan analysis.

B) Crystal Ball Efficiencies, Resolution and "Baseline" Measurements

As an introduction to the use of these inclusive distributions in a scan, we will discuss the efficiencies and resolution for each particle type, and then look at sample distributions taken at the psions or off-resonance/below charm threshold ($\sqrt{s}$ = 3670). These show the baseline characteristics of the spectra where no D's are present. Then we use the spectra at $\psi''(3770)$ to see if a D-rich final state

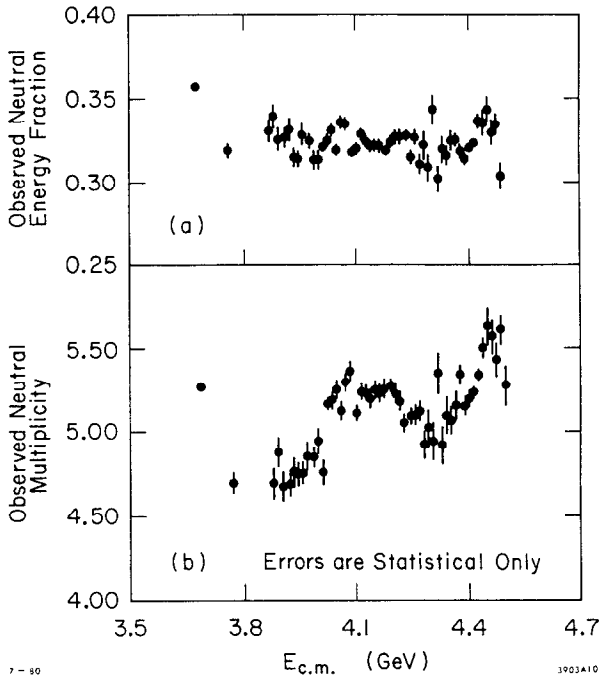

Fig. 10. Inclusive Quantities in the Crystal Ball Scan Mode: a) Neutral energy fraction, b) Neutral Multiplicity (Ref. 19).

distorts the baseline measurement. The ψ'' then often serves as a background curve for the remainder of the scan region.

1) Hadronic cross section: The most basic distribution is R vs $\sqrt{s}$, obtained from the calorimetric properties of the Ball. A simple energy threshold is inadequate to separate hadrons, so cuts on the spatial distribution of energy and track topologies are introduced. The results[19] are additionally τ-subtracted and background subtracted. Radiative corrections depend critically on the structures present and have not been applied to samples in this report. At this juncture we estimate that there may be a 15% absolute systematic error on the average R measured in a local region of $\sqrt{s}$, and a point-to-point systematic of ±5% around this average. Our baseline result for R is

$$R(\sqrt{s} = 3670 \text{ MeV}) = 2.4 \pm .3$$

2) Photons: We have already given the energy and angular resolutions. NaI(Tℓ) has essentially no intrinsic inefficiency for photons of energy > 20 MeV (our software cutoff). Effective inefficiencies are introduced by cuts to avoid overlap of photons with other particles. A precise absolute photon energy calibration can be maintained by interspersing data runs at the ψ', where the observed χ-lines test the overall calibration to $\sim \pm 1$ MeV. As a guide for how monochromatic γ's will appear in inclusive spectra we show Fig. 11, the photon spectrum from ψ' as observed in the counting room after three hours of data acquisition (10.5 nb^{-1}).

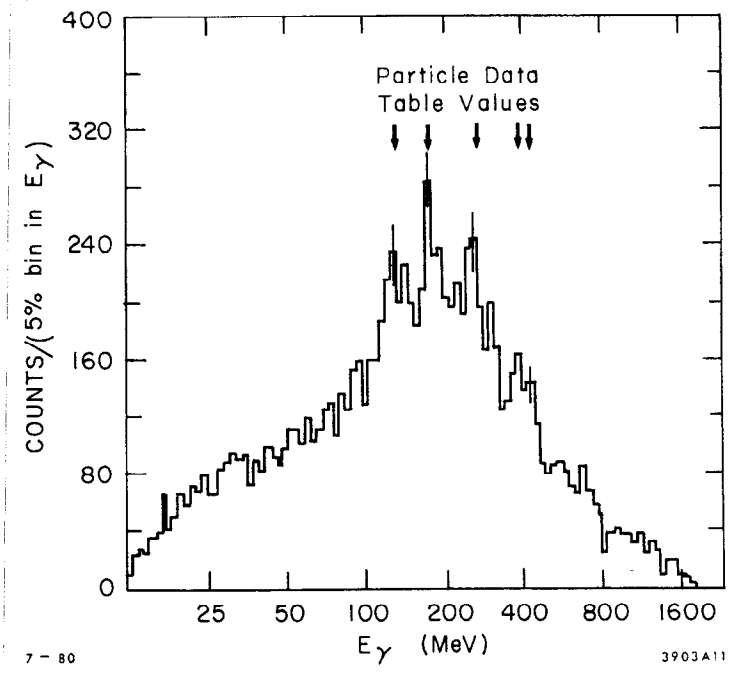

Fig. 11. Counting room appearance of γ peaks from $\psi \to \chi + \gamma$ after small samples characteristic of a scan.

This tiny sample has been so chosen to give the same absolute signal in each peak as would a resonance $F^* \to \gamma F$ produced with $\Delta R = 1$ and $B_\gamma = 100\%$, where the hypothetical run would last $\sim \frac{1}{2}$ day. (The peak would have two to four times less background under reasonable assumptions).

The low-energy photon spectra actually obtained below charm threshold (3670) and at ψ'' are unremarkable: Fig. 12 shows the "baseline" distribution at ψ''. Note that the choice of a $\ell n E\gamma$ scale transforms the spectrum so that the prominent peak at $m_\pi/2 \approx 70$ MeV which we see in a linear plot (arising from $\pi^0 \to \gamma\gamma$) completely disappears. This means that any π^0-related bump appearing on this type of spectrum near 70 MeV signals an excess of low energy π^0's over the normal population. The value $E_\gamma \approx 200$ MeV is significant in that minimum ionizing charged particles masquerading as photons would produce a peak here.

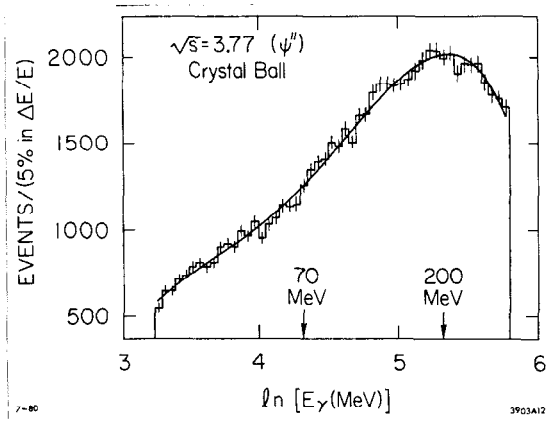

Fig. 12. The inclusive γ energy-spectrum of the ψ'' as obtained by the Crystal Ball.

3) π^0: A global reconstruction for π^0's is used in which each photon is used in at most one π^0 and in which the goodness of fit reflects the total hypothesis for assignments of γ's to π^0's. The efficiency for π^0 reconstruction is $\leq 60\%$, where there is a marked dependence on the severity of topological cuts (such as overlap). The momentum distribution of resulting π^0's is relatively unbiased because the NaI is sensitive to low-energy γ's. From measurements at the ψ, the mass resolution is $\sigma/m_\pi \approx 4\%$, but this depends sharply on the π momentum distribution. In the scan, π^0 selection effectively picks out $m_{\gamma\gamma} = m_{\pi^0} \pm 15\%$. The angular resolution of the π^0 is such as to permit meaningful angular distributions ($\Delta\cos\theta \approx .1$) down to π^0 momenta of ~20 MeV/c.

The π^0 total energy "baseline" spectrum for the ψ'' is shown in Fig. 13. Again, this spectrum is devoid of features; note the very

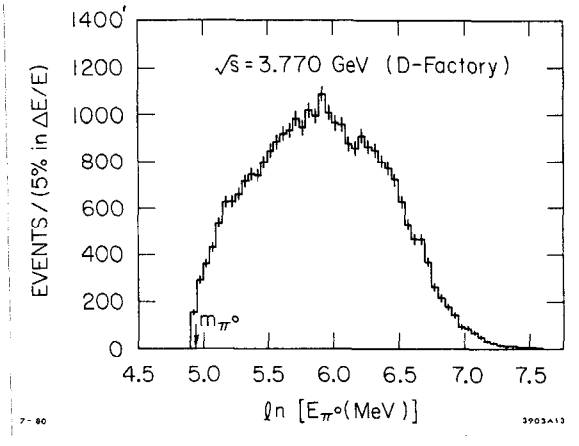

Fig. 13. The inclusive π^0 total-energy spectrum of the ψ'' (Crystal Ball).

smooth rise from m_{π^0}. In these π^0 energy spectra, the π^0 mass is constrained to the usual value after the global assignment of γ's to π^0: this has the effect of adjusting the γ energies and opening angle to more precisely determined values.

4) $\underline{\eta^0}$: The efficiency for detection of the decay $\eta \to \gamma\gamma$ is about 30% after all topological cuts. The resolution for the total inclusive η signal observed in the scan is $\sigma/m_\eta = 4\%$ (see later discussion in Section V.C and Fig. 24). An improvement in the signal:background for η's can be gained from π^0 subtraction or from energy/topology cuts (requiring mainly $m_\gamma > 140$ MeV and particle multiplicities between two and six for charged and neutrals separately--the so-called DASP cuts). Such improvements decrease the efficiency and introduce larger errors in the calculation of the efficiency.

It is something of a surprise to see how weakly a reasonable η-signal should appear in an $m_{\gamma\gamma}$ plot. Figure 14 shows a very large data sample taken at the ψ, where the average number of η's/event is about 1/4. The η signal is quite evident, but only by virtue of the good statistics (note the error bars). It behooves us to find cuts clearly defining the η for use in less abundant data sets. Figure 15 shows the upper end of this same sample, with π^0 subtraction, and Fig. 16 shows it with the DASP cuts but no π^0 subtraction. Both techniques work, but the former is better statistically for the Ball and is less biasing.

We now consider the "baseline" η measurements at $\sqrt{s} = 3670$ (off-ψ') and at the D-factory $\psi''(3770)$. There are clear (and strong) η signals at both points. Figure 17a,b show these results in the π^0-subtracted plots. Fits were made to both the unsubtracted and π^0-subtracted data, with the answers in close agreement after efficiency

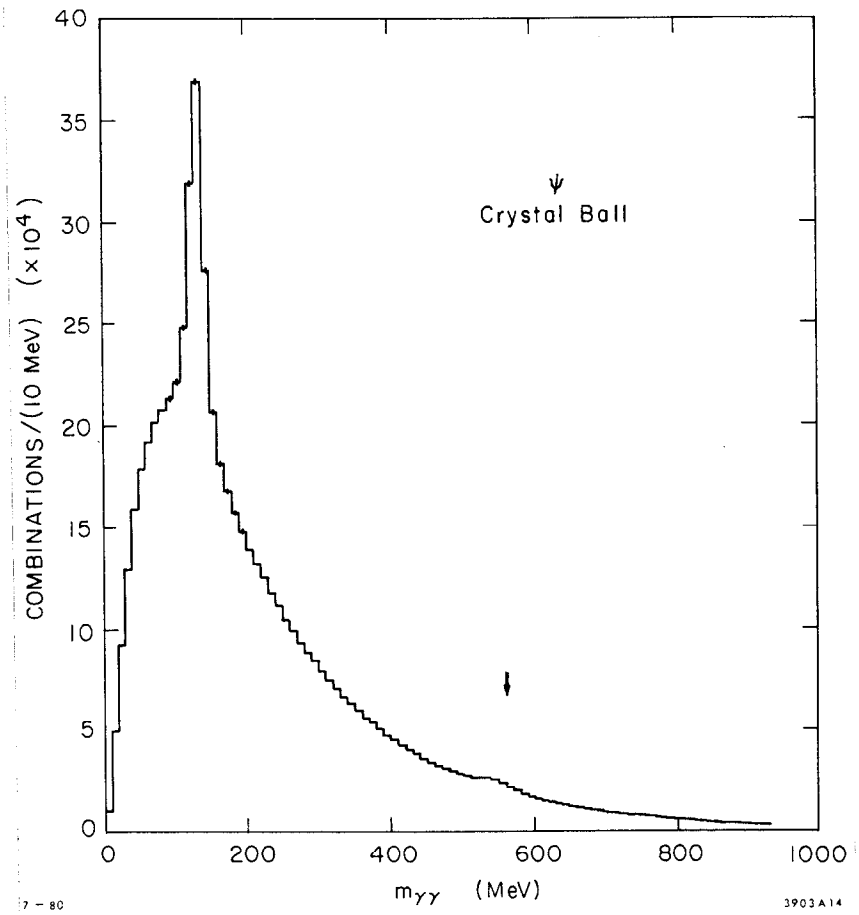

Fig. 14. The distribution of $m_{\gamma\gamma}$ for all photons detected inclusively at the ψ (Crystal Ball).

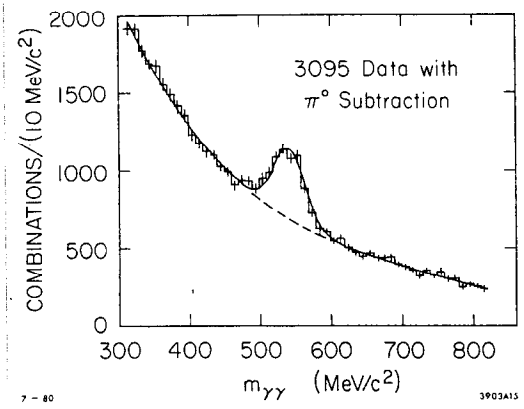

Fig. 15. The π^0-subtracted $m_{\gamma\gamma}$ spectrum of Fig. 14.

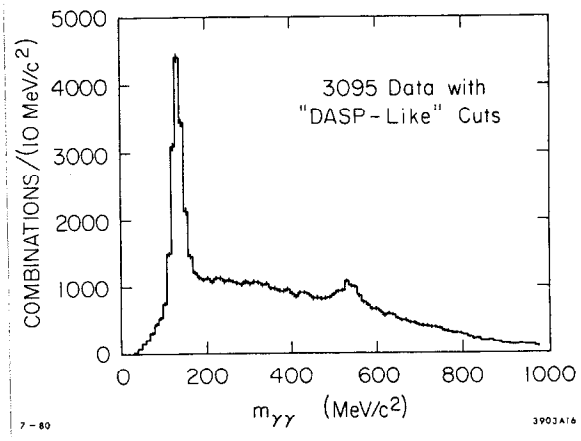

Fig. 16. The DASP-cut $m_{\gamma\gamma}$ spectrum of Fig. 14.

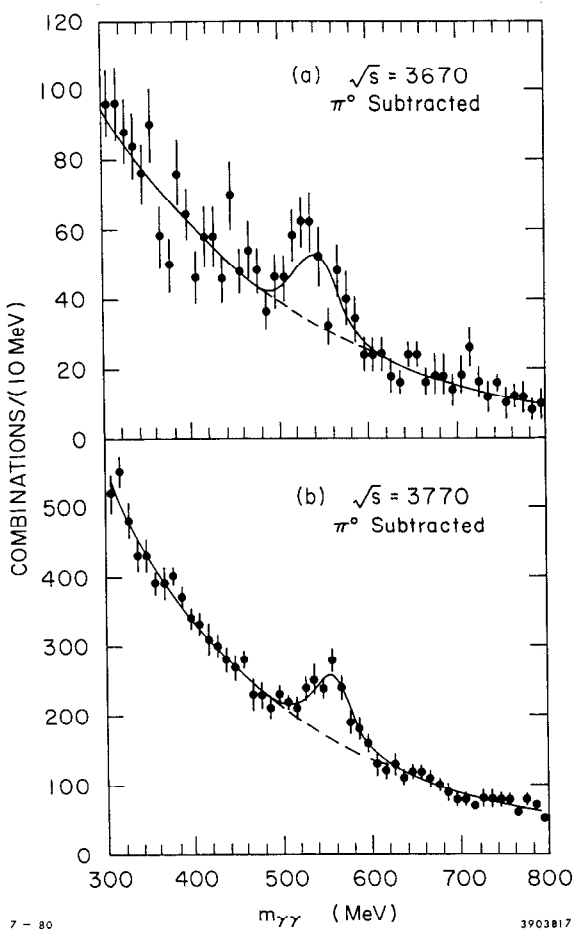

Fig. 17. Eta signals in the Crystal Ball:
a) at $\sqrt{s}$ = 3670 MeV;
b) at $\sqrt{s}$ = 3770 MeV.

corrections (see Section V.C for more detail about the fits). At $\sqrt{s}$ = 3670 we get f_η = .28 ± .06 and at the ψ'', f_η = .16 ± .03 [$R_\eta = f_\eta \cdot R$].

The baseline measurements for γ, π^0 energy and inclusive η have thus been established, with little structure seen for γ and π^0 at and below ψ'' (except for ψ', of course). The strong non-charmed production of η's even compared to ψ'' implies that the old physics can be a major source of η's in the scan region. The ψ'' value shows that D's may also have substantial decay modes involving η's.

V. CRYSTAL BALL RESULTS FOR $\sqrt{s}$ > 3.9 GeV

After this long preparation, we can now discuss the available spectra in the regions most crucial to the physics outlined in Section III.

A) Preliminary Results for R.

Data from the 5-week initial scan (Table I) have been analyzed for R, and the results[19] are displayed in Fig. 18 (note suppressed zero). Even for this small sample the systematics greatly dominate the statistical errors. The usual qualitative picture is confirmed, with clear 3.77, 4.03 and 4.4 peaks. The 4.16 region is consistent with one broad structure if the ±5% point-to-point systematic errors are assumed to be present at their extreme. A less conservative interpretation is that the structure near 4.05 - 4.20 may be more

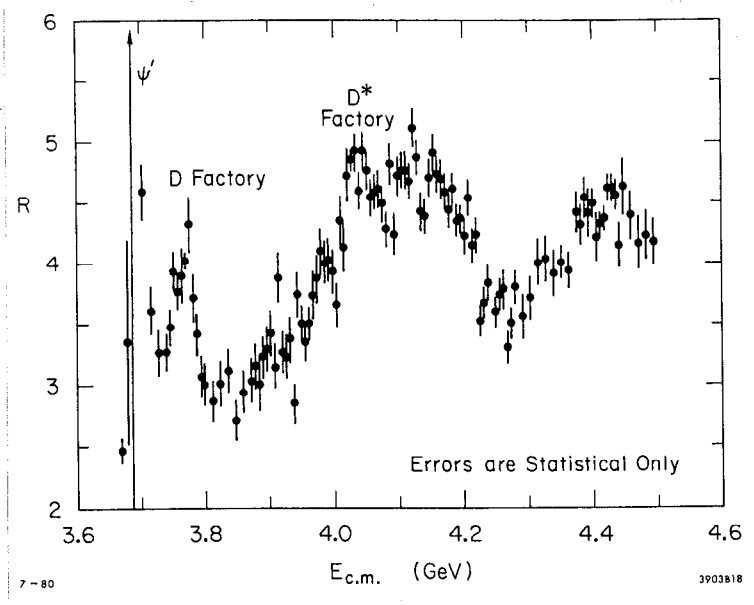

Fig. 18. The behavior of R through the Crystal Ball Scan Region [τ- and background-subtraction have been made but not radiative corrections] (Ref. 19).

complex. Similar fluctuations are present in the sharp rise from 3.9 to 4.03 GeV. The "valley" region 4.2 - 4.3 GeV shows no localized narrow peaks, but the data are not sensitive to the smoothly distributed .2 - .3 units of R predicted in Fig. 8. With the entire data sample (Table I) the statistical precision will be very high, but it is not yet clear that point-to-point systematic error can be reduced enough to exploit the large sample.

B) Results at $\sqrt{s}$ = 4.028 GeV ("D^*-Factory").

The main thrust of the data gathered at this copious source of D^*'s is to refine the parameters related to production and decay of these states. It should be stressed that there are two major independent measures of these quantities: the inclusive, completely π^0-subtracted γ energy spectrum and the pure π^0 energy spectrum. However, because π^0 separation is never complete, the plots will be somewhat correlated. We choose to fit unsubtracted γ and π^0 spectra for the parameters separately, and quote the best results (not averages).

1) The γ energy spectrum for well-measured photons is shown in Fig. 19 (complete data sample). Prominent peaks appear at ~70 and ~135 MeV, with widths corresponding to the Doppler broadening for γ's from π^0's of kinetic energy ~6 MeV (for the lower peak) and to the recoil-shifted, Doppler- and resolution-broadened photon transition

$D^* \to \gamma D$ (upper peak). The effect of (partial) π^0 subtraction is shown in Fig. 20, where the lower peak almost disappears. Figure 21 shows

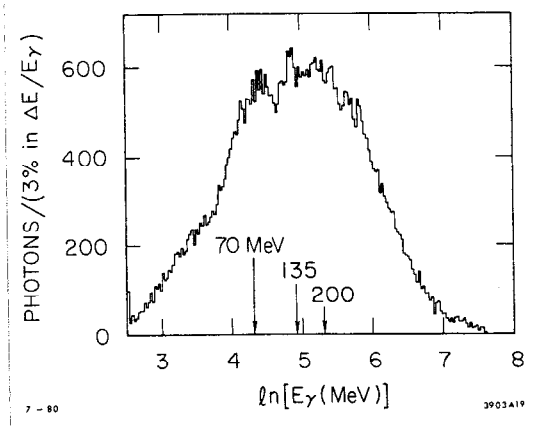

Fig. 19. Inclusive energy spectrum at $\sqrt{s}$ = 4028 MeV from the Crystal Ball.

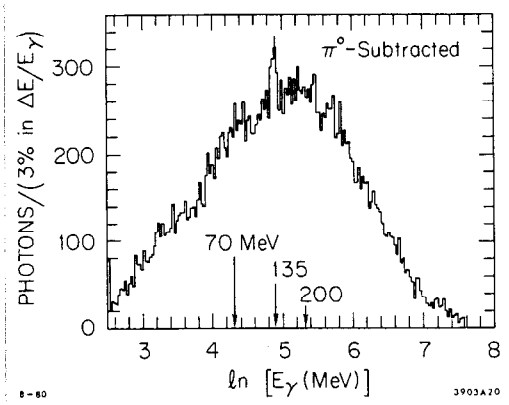

Fig. 20. The π^0-subtracted γ spectrum of Fig. 19.

the details of a multi-parameter fit to this spectrum, where the smooth background is taken from the ψ'' result and the shapes of the bumps from Monte Carlos (checked for effects of resolutions, interactions, inefficiencies and real analysis programs). The variable parameters are the D and D* masses, the peak/background ratio, the $D^*\bar{D}^*$:$D^*\bar{D} + D\bar{D}^*$ ratio and the branching ratio of the radiative transition B_γ. Although transitions of neutral D's dominate these numbers, we delete the superscript "o" whenever the fits really measure a sum of neutral and charged D transitions. The results of this particular fit are shown in Table II. Similar fits with variation of cuts, backgrounds and Monte Carlo parameters were done to test the systematic errors. Best values with systematics attached from these and following fits will be shown in Table III.

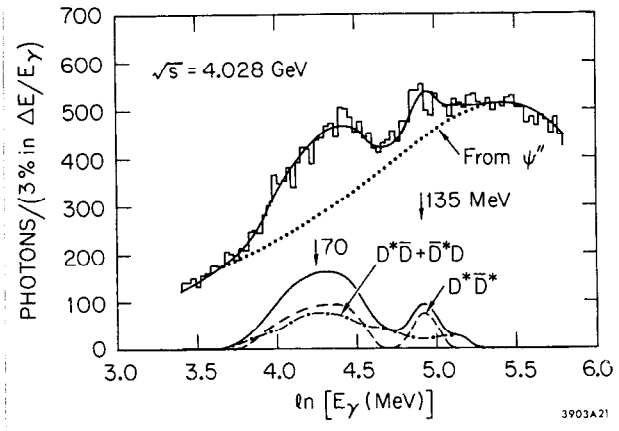

Fig. 21. Components of a fit to the spectrum of Fig. 19.

Table II: Results of a typical fit to the γ-energy spectrum at $\sqrt{s}$ = 4028 MeV

$m_{D^0} = 1863 \pm 2$ MeV
$m_{D^{*0}} = 2005 \pm 2$
$B_\gamma = 32 \pm 2\%$
$D^*\bar{D}^*:D^*\bar{D} + D\bar{D}^* = 1:1.9 \pm .4$

2) The π^0 energy spectrum can be obtained with or without π^0 candidates constrained to the π^0 mass. Fig. 22, the former spectrum, distinctly shows that the broad bump seen in the γ spectrum (Fig. 19) is really very monochromatic, almost stationary π^0's. (Note that here the $\ell n\ E_{\pi^0}$ scale is used to spread the peak out to render it distinguishable from $E_{\pi^0}=m_{\pi^0}$!). The dramatic change from the ψ" spectrum assures us that a change from unexcited charm states has occurred. The detailed shape of the spectrum is again very sensitive to the $D^*\bar{D}^*:D^*\bar{D}+D\bar{D}^*$ ratio (because 4028 MeV is ~16 MeV above the first threshold and ~160 MeV above the second). It is also the most sensitive measure of the Q-value $m_{D^{*0}} - m_{D^0}$ because of the spreading of the portion of the spectrum

Table III: Best Values of the D/D* Production/Decay Parameters[a]

Measurement	C.B. Value	Previous Best Value[b] (Mark I)
m_{D^0}	1864 ± 2 MeV	1863.3 ± 0.9 MeV
$m_{D^{*0}}$	2005 ± 2 MeV	2006 ± 1.5 MeV
$BR(D^* \to \gamma D)$	31 ± 6%	45 ± 15% (for neutral D's)
$Q(D^{*0} \to \gamma D^0)$	142.2 ± 2 MeV	142.7 ± 1.7
$D^*\bar{D}^*:D^*\bar{D} + D\bar{D}^*$	1:1.95 ± .35 ± .7	1:0.95 ± .15 (for neutral D's)

a Errors include systematics.
b See Ref. 8.

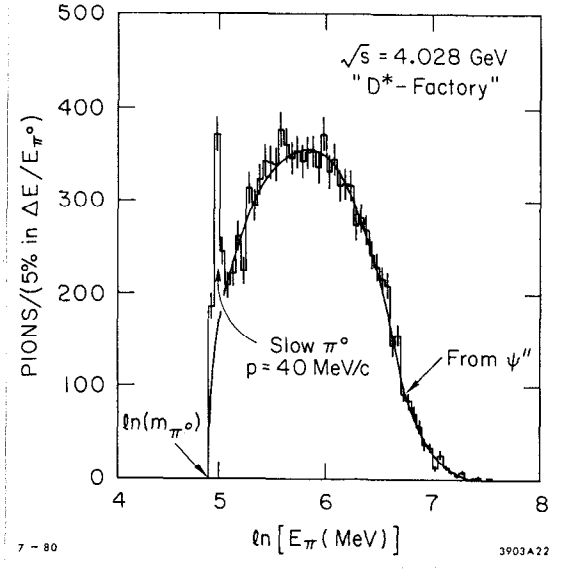

Fig. 22. The π^0 total energy spectrum of the Crystal Ball at $\sqrt{s}$ = 4028 MeV with π^0 candidates constrained to m_{π^0}.

derived from $D^*\bar{D}^*$, though this is correlated to the above ratio. An example of the details of this slow π^0 peak, this time from the sample with the π^0 unconstrained to m_{π^0}, is given in Fig. 23. The fits are good and yield parameters consistent with the other two data sets, though with larger errors.

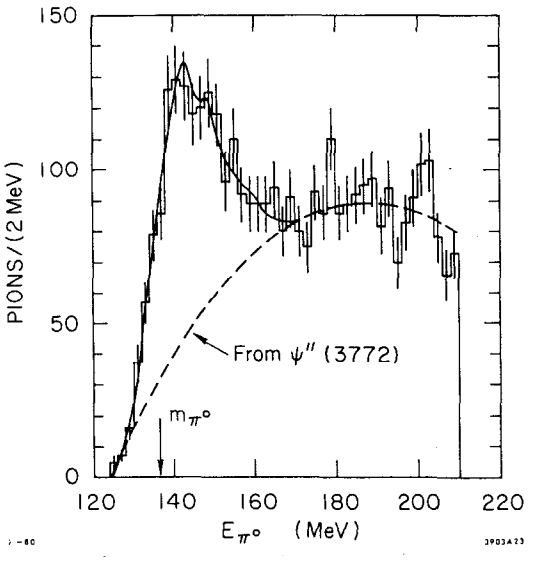

Fig. 23. Details of the slow π^0 energy spectrum, without the π^0 mass constraint of Fig. 22.

Table III gives our best estimates of the parameters of the D^* production and decay as gleaned from the above analysis. The masses have been determined at a level comparable to previous experiments and are consistent. The Q-value is also consistent with the Mark I value and has a similar error; in our data this error is almost entirely systematic. The branching ratio $B_\gamma = 31.0 \pm 6\%$ has been determined much more precisely by this first direct measurement of the transition γ; the error is again almost all systematic. There is a hint of disagreement in the new and old values of the production ratios of D^*'s; although covered by the errors, our independent plots consistently show $D^*\bar{D}^*$ to be a weaker effect than D^*D modes. The Mark I measurement must however be considered a more direct measure at this time. We are investigating the possibility of tagging one slow π^0 and looking at the absolute content of γ and π^0 peaks of the event, a technique which is a direct measure of the proportion of the two modes.

Discussion of the η-inclusive rate at 4.028 is included in the next section.

C) Results of the Inclusive-η Measurement for $3.86 < \sqrt{s} < 4.5$ GeV

A search for F, F^* and F^{**} mesons entails examination of inclusive γ, η and possibly π^0 spectra over the entire scan region. We report here only the inclusive η measurements, and for η's, only an examination in broad steps in $\sqrt{s}$. This facilitates comparison with previous results, but leaves as an open question the possibility of small local enhancements.

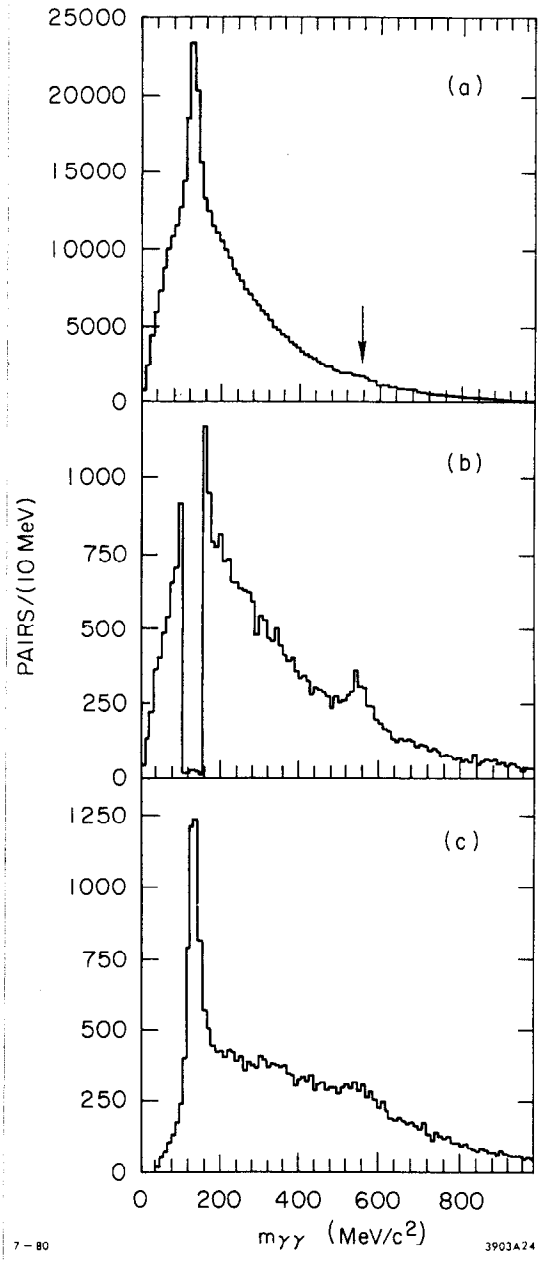

Fig. 24. The $m_{\gamma\gamma}$ mass distribution summed over $3.86 < \sqrt{s} < 4.5$ GeV: a) total sample; b) π^0-subtracted; c) DASP cuts (on Crystal Ball data).

The combined data sample from $3.86 < \sqrt{s} < 4.5$ GeV (1979 data only) shows characteristic η peaks in the $m_{\gamma\gamma}$ distribution as shown in Fig. 24 for the different cuts described earlier. Again, π^0-subtracted plots show the signal best, but both subtracted and unsubtracted plots are used for the fits to estimate systematics. The data are divided into segments closely approximating the choice made by DASP,[10] and fits are performed on each segment. Parameters of the fit are the background shape and amplitude, the η mass, width and amplitude; we find close agreement in the η mass and width in these fits compared to those at ψ'' and elsewhere. The fitted amplitude is translated into an effective number of η's produced by correcting

for the detection efficiency (again by Monte Carlo calculation as described earlier) and branching ratio for $\eta \to \gamma\gamma$. Then f_η = (number of effective η)/(number of hadronic events) is the average number of η's/hadronic event. f_η has the advantage of relatively stable behavior in $\sqrt{s}$ although R may oscillate widely at resonances. Of course $\sigma_\eta \equiv R_\eta \sigma_{\mu\mu} = f_\eta R \sigma_{\mu\mu}$ may be used to obtain absolute cross sections.

The preliminary excitation function for f_η is shown in Fig. 25, including values obtained on/off resonances. The numerical values are given in Table IV. The overall systematic error is unknown, but the point-to-point errors are likely dominated by statistics. Previous values, where available, are also shown in both the Figure and Table, where we have used R,[4] σ_η,[10] given by DASP to calculate their f_η. (Limits are 1 - s.d.)

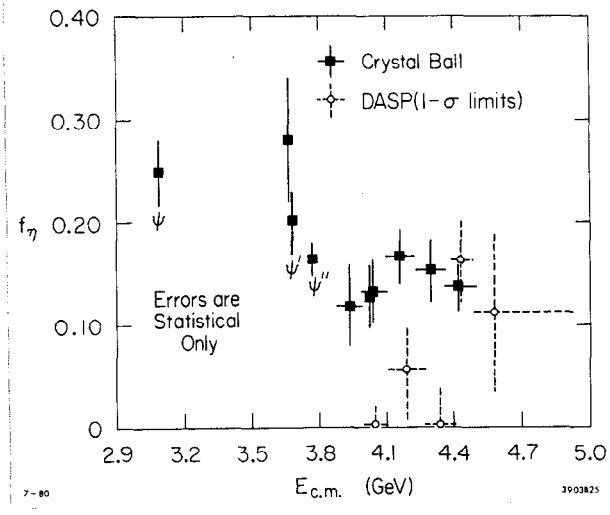

Fig. 25. The excitation of f_η as a function of $\sqrt{s}$: Crystal Ball scan and resonance measurements are solid lines; DASP scan measurements are dashed.

The trend set by our baseline measurements continues, in that f_η remains large and constant within the errors. We see no evidence that η production shows the thresholds associated with F-production suggested by previous measurements. This rules out neither smaller local η enhancements

Table IV: Values for f_η as a Function of $\sqrt{s}$: Crystal Ball Scan and Resonance Measurements

c.m. Energy Range in GeV	f_η	
	C. B. Value	Previous Best Value (DASP) [a]
3.670	.28 ± .06	none
3.86 - 4.0	.12 ± .04	none
4.0 - 4.1	.13 ± .03	< .02
4.1 - 4.28	.17 ± .03	.05 ± .05
4.28 - 4.38	.15 ± .03	< .04
4.38 - 4.5	.14 ± .02	.16 ± .04

[a] See Ref. 10

nor does it rule out the evidence for F, F^* via exclusive kinematic fits in these regions. A subtraction of the noncharmed background is now possible in principle, but awaits amalgamation of the complete sample at $\sqrt{s}$ = 3670 MeV and better control of the systematic errors. The gentle rise of f_η in the R-valley ($\sim$4.25 GeV) can easily be attributed to a higher f_η (non-charm) than f_η (charm) and the diminution of the charm signal in the valley; we do not need to invoke F signals to explain the data.

ACKNOWLEDGEMENTS

I would like to acknowledge the value of the close cooperation in the management of the continuum scan by my colleague H. F. W. Sadrozinski, but even more, his leadership of the analysis effort which resulted in most of the new physics results in this report.

We also greatly appreciate the special efforts added to this project by D. G. Aschman, M. Joy, G. I. Kirkbride, F. C. Porter, J. C. Tompkins and the Operations Staffs at SPEAR and SLAC.

This report has been supported in part by the Department of Energy, contract DE-AC03-76SF00515, and in part by National Science Foundation Grant PHY79-16461.

APPENDIX

STATUS OF THE η_c CANDIDATE

The major thrust of this report was to introduce the reader to use of the Crystal Ball in the continuum. For completeness, we update another result of topical interest; the η_c candidate (2980 MeV) detected[19b] by the Crystal Ball operating in an inclusive mode. The evidence for the transitions $\psi' \to \gamma\eta_c$ and $\psi \to \gamma\eta_c$ are shown in Fig. 26, where the raw and background-subtracted inclusive γ energy spectra are shown. The new state is determined to be at 2980 $\pm$ 16 MeV from both sets of data independently; the joint fit value is 2980 $\pm$ 15 MeV. There is no useful η_c width information in the ψ' data because 8% (FWHM) resolution on a $\sim$600 MeV γ yields 50 MeV resolution width. At the ψ, 12% (FWHM) on $\sim$110 MeV γ yields absolute resolutions of $\sim$13 MeV. Fits to this spectrum yield an intrinsic width $\sim$20 MeV, but the error is so large that this is less than two s.d. from an intrinsic width of zero, and even more consistent with a

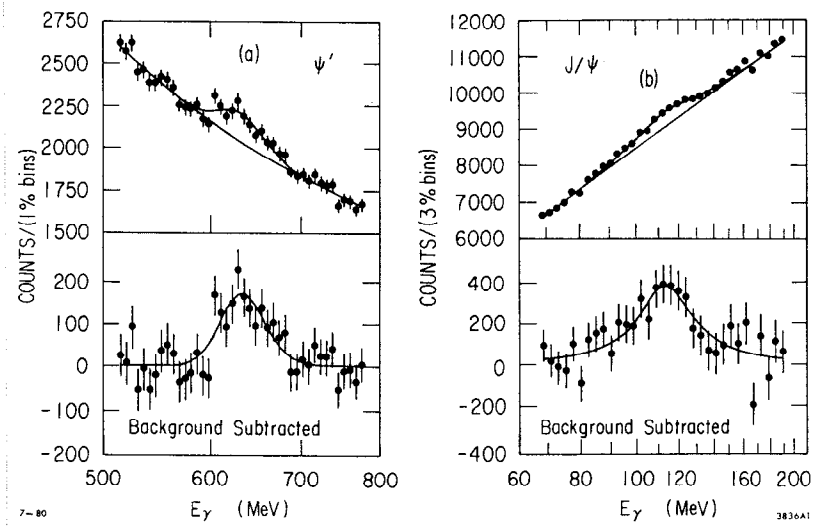

Fig. 26. Inclusive energy spectra from the Crystal Ball: a) $\psi' \to \gamma$ + all; b) $\psi \to \gamma$ + all.

conjectured value of 5 MeV often quoted.[20] Clearly, the η_c width has not yet been measured.

Subsequent to this result, evidence for the $\eta_c(2980)$ in exclusive channels has been found; first by the SLAC/LBL Mark II group[21,22] and shortly after by the Crystal Ball group.[23] The exclusive channels are different: Mark II sums the channels

$$\psi' \to \gamma + \begin{cases} K^{\mp}K^{0}_{S}\pi^{\pm} \\ K^{+}K^{-}\pi^{+}\pi^{-} \\ \pi^{+}\pi^{-}\pi^{+}\pi^{-} \\ p\bar{p} \\ p\bar{p}\,\pi^{+}\pi^{-} \end{cases}$$

(dominated by $\psi' \to (K^{\pm}K^{0}_{S}\pi^{\mp}) + \gamma$) while the Crystal Ball looks at the pure channel $\psi \to (\eta\pi^{+}\pi^{-}) + \gamma$. The fits to these channels are 1C/5C† and 3C, respectively. These new results are shown in Fig. 27 and 28.

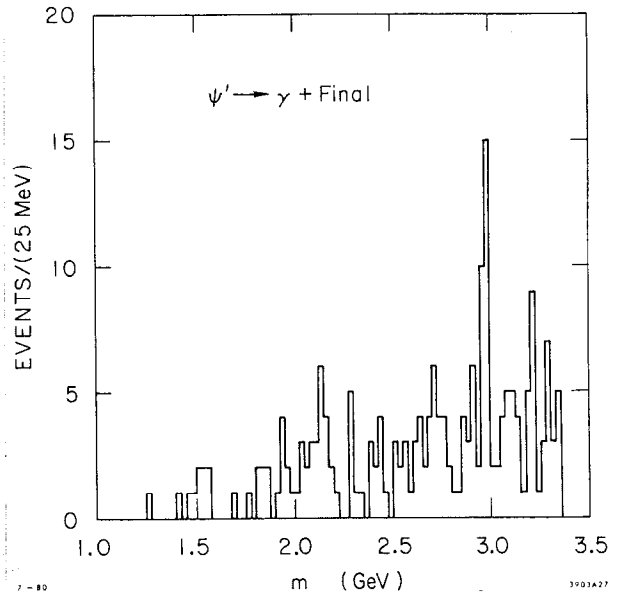

Fig. 27. The m_{final} distribution for the candidates $\psi' \to \gamma\eta_c$, $\eta_c \to$ final.

† The analyses from Ref. 21, 22, and 24 differ.

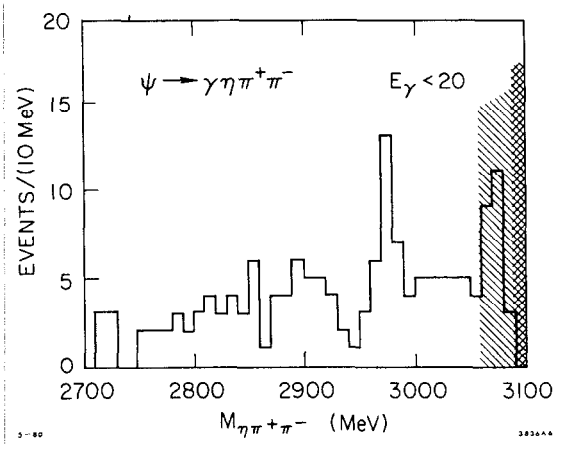

Fig. 28. The $m_{\eta\pi^+\pi^-}$ distribution for the candidates
$\psi \rightarrow \eta_c\gamma$
$\hookrightarrow \eta\pi^+\pi^-$

The significance of each peak is >4 s.d. For detailed discussion of these results, see Bloom.[24] The branching fractions, both $\psi/\psi' \rightarrow \eta_c\gamma$ and $\eta_c \rightarrow$ final state, are estimated, but only the product ratios $\psi/\psi' \rightarrow \gamma$ + final state are anything but rough guesses. Table V gives these estimates.

Table V: Estimates and Comparisons of the Product and Single Branching Ratios from $\psi/\psi' \rightarrow \eta_c\gamma$ and $\eta_c \rightarrow$ Final States

Property	Crystal Ball	Mark II
Measurements:		
Mass	2980 ± 15 MeV	2978 ± 8 MeV
Natural Full Width	< 35 (consistent with 0 to 20)	< 30 MeV
$BR(\psi' \rightarrow \gamma\eta_c)BR(\eta_c \rightarrow \pi^\pm K^\mp K_S)$	- - -	$1.5 \pm .6 \times 10^{-4}$
$BR(\psi \rightarrow \gamma\eta_c)BR(\eta_c \rightarrow \eta\pi^+\pi^-)$	$2.7 \pm 1.5 \times 10^{-4}$	- - -
$BR(\psi \rightarrow \gamma\eta_c)BR(\eta_c \rightarrow \gamma\gamma)$	$< 4 \times 10^{-5}$ (90% C.L.)	- - -
Rough Indications:		
$BR(\psi' \rightarrow \gamma\eta_c)$	~ .5%	- - -
$BR(\psi \rightarrow \gamma\eta_c)$	~ 1%	- - -
Implications:		
$BR(\eta_c \rightarrow \pi^\pm K^\mp K_S)$	- - -	~ 3%
$BR(\eta_c \eta\pi^+\pi^-)$	~ 3%	- - -
$BR(\eta_c \rightarrow \gamma\gamma)$	~ .4%	- - -

REFERENCES

1. Members of the Crystal Ball collaboration. California Institute of Technology, Physics Department: R. Partridge, C. Peck and F. Porter. Harvard University, Physics Department: A. Antreasyan, Y. F. Gu, W. Kollmann, M. Richardson, K. Strauch and K. Wacker. Princeton University, Physics Department: D. Aschman, T. Burnett (visitor), M. Cavalli-Sforza, D. Coyne, M. Joy and H. Sadrozinski. Stanford Linear Accelerator Center: E. D. Bloom F. Bulos, R. Chestnut, J. Gaiser, G. Godfrey, C. Kiesling, W. Lockman and M. Oreglia. Stanford University, Physics Department and High Energy Physics Laboratory: R. Hofstadter, R. Horisberger, I. Kirkbride, H. Kolanoski, K. Koenigsmann, A. Liberman, J. O'Reilly and J. Tompkins.
2. R. Partridge et al., Phys. Rev. Lett. 44, 712 (1980); Y. Chan et al., IEEE Transactions on Nuclear Science, Vol. NS-25, No. 1. 333 (1978); I. Kirkbride et al., IEEE Transactions on Nuclear Science, Vol. NS-26, No. 1, 1535 (1979).
3. E. D. Bloom, in Proceedings of the XIVth Rencontre de Moriond, Les Arcs, France, ed., j. Tran Than Van (1979).
4. J. L. Siegrist, "Hadron Production by e^+e^- Annihilation at Center-or-Mass Energies between 2.6 and 7.8 GeV," SLAC Report 225, p. 75, Oct. 1979.
5. P. A. Rapidis, "D Meson Production in e^+e^- Annihilation," SLAC Report 220, p. 81, June 1979.
6. R. H. Schindler, "Charmed Meson Production and Decay Properties at the psi(3770)," SLAC Report 219, Ph.D Thesis, May 1979.
7. G. S. Abrams et al., " Observation of Cabibbo Suppressed Decays $D^0 \to \pi^+\pi^-$ and $D^0 \to K^+K^-$," Phys. Rev. Lett. 43, 481 (1979); also SLAC-PUB-2337 (May 1978).
8. G. Goldhaber, "The Spectroscopy of New Particles," LBL Report 6732, P. 13, Aug. 1977.
9. G. J. Feldman, "Charmed Particle Spectroscopy," SLAC-PUB-2068, Dec. 1977.
10. R. Brandelik et al., Phys. Lett. 70B, 132 (1977).
11. R. Brandelik et al., Phys. Lett. 80B. 412 (1979).
12. C. Quigg and J. Rosner, Fermilab Pub 77/60-TH(1977).
13. R. Ammar et al., Preprint PRINT-80-0338 (Kansas), 1980; to be published in Phys. Lett.; and R. Kumar in Proceedings of the VIth International Conference on Experimental Meson Spectroscopy, (Brookhaven National Laboratory, Upton, N.Y., 1980), ed. S. U. Chung, to be published.
14. A. De Rújula, H. Georgi, S. L. Glashow, Phys. Rev. Lett 37, 785 (1976).
15. E. Eichten, K. Gottfried, T. Kinoshita, K. D. Lane, T. M. Yan, Phys. Rev. D17, 3090 (1978) and CLNS-425 (June 1979).
16. K. Gottfried, in an invited talk at the 1980 Vanderbilt Symposium (in remarks on subjects not to be discussed).
17. R. Cahn and B. Kayser, "Angular Distributions and the Physics of Charmed Meson Production at the 4.028 GeV Resonance," LBL-10692 (1980); Also see A. De Rújula, H. Georgi, S. L. Glashow, Phys. Rev. Lett. 37, 398 (1976).
18. J. L. Siegrist, Op. Cit., p. 39-41.

19. a) J. C. Tompkins, "Recent Results from the Crystal Ball," SLAC Report 224, 578 (1980).
b) E. D. Bloom, Proceedings of the 1979 International Symposium on Lepton and Photon Interactions at High Energies, Aug. 23-29, 1979, Fermilab; SLAC-PUB-2425 (1979).
20. T. Appelquist, R. M. Barnett, K. D. Lane, "Charm and Beyond," Ann. Rev. Nucl. Part. Sci. 28 (1978); also SLAC-PUB-2100 (1978).
21. T. M. Himel, "Decays of the $\psi'(3684)$ to Other Charmonium States," SLAC Report 223, Oct. 1979.
22. G. Trilling, D. Scharre, private communication.
23. D. G. Aschman, "Radiative Decays of ψ and ψ'," SLAC-PUB-2550, (1980) (to be published in Proceedings of the XV Rencotre de Moriond, Les Arcs, France, March 15-21, 1980).
24. E. D. Bloom, "Radiative Transitions to an $\eta_c(2980)$ Candidate State and the Observation of Hadronic Decays of this State," SLAC-PUB-2530 (1980).